

# The Archaeal Histone-Fold Protein HMf Organizes DNA into Bona Fide Chromatin Fibers

Miroslav Tomschik,<sup>1,4,5</sup> Mikhail A. Karymov,<sup>1,4,6</sup>  
Jordanka Zlatanova,<sup>2,3</sup> and Sanford H. Leuba<sup>1,3</sup>

<sup>1</sup>Physical Molecular Biology  
Laboratory of Receptor Biology  
and Gene Expression  
National Cancer Institute  
National Institutes of Health  
41 Library Drive, Room B507, MSC 5055  
Bethesda, Maryland 20892

<sup>2</sup>Department of Chemistry  
and Chemical Engineering  
Polytechnic University  
6 MetroTech Center  
Brooklyn, New York 11201

## Summary

**Background:** The discovery of histone-like proteins in Archaea urged studies into the possible organization of archaeal genomes in chromatin. Despite recent advances, a variety of structural questions remain unanswered.

**Results:** We have used the atomic force microscope (AFM) with traditional nuclease digestion assays to compare the structure of nucleoprotein complexes reconstituted from tandemly repeated eukaryal nucleosome-positioning sequences and histone octamers, H3/H4 tetramers, and the histone-fold archaeal protein HMf. The data unequivocally show that HMf reconstitutes are indeed organized as chromatin fibers, morphologically indistinguishable from their eukaryal counterparts. The nuclease digestion patterns revealed a clear pattern of protection at regular intervals, again similar to the patterns observed with eukaryal chromatin fibers. In addition, we studied HMf reconstitutes on mononucleosome-sized DNA fragments and observed a great degree of similarity in the internal organization of these particles and those organized by H3/H4 tetramers. A difference in stability was observed at the level of mono-, di-, and triparticles between the HMf particles and canonical octamer-containing nucleosomes.

**Conclusions:** The *in vitro* reconstituted HMf-nucleoprotein complexes can be considered as bona fide chromatin structures. The differences in stability at the mono-particle level should be due to structural differences between HMf and core histone H3/H4 tetramers, i.e., to the complete absence in HMf of histone tails beyond the histone fold. We speculate that the existence of core

histone tails in eukaryotes may provide a greater stability to nucleosomal particles and also provide the additional ability of chromatin structure to regulate DNA function in eukaryotic cells by posttranslational histone tail modifications.

## Introduction

Ever since the three domain concept of life was forwarded [1], scientists have been trying to understand the basic characteristic features of organisms belonging to the new domain Archaea, and to figure out how these distinct living creatures may have evolved. Cytologically Archaea may be considered prokaryotic, since they lack nucleus, cytoskeleton, and organelles. At the molecular level, however, Archaea have some features that put them close to prokaryotic organisms (metabolism, for example), while other features (such as information processing) are more similar to those of eukaryotes. The latter similarities have suggested that Archaea and Eukarya have a common evolutionary ancestor. The question was raised of whether the archaeal genome is organized in the form of chromatin, as is the nuclear genome in eukaryotes.

The formulation of the Archaea “chromatin” concept came from several lines of experimental evidence: the presence of histone-like proteins, electron microscopy and nuclease-digestion studies of nucleoprotein fibers isolated from cells, and finally, from *in vitro* reconstitution experiments in which naked DNA fragments were combined with purified archaeal histones (reviewed in [2, 3]).

A family of archaeal proteins closely resembling eukaryal histones has been described [4, 5]. These proteins are strongly conserved among themselves and share strong sequence similarities with the folded regions of the eukaryal core histones. Secondary structure predictions [6, 7] and actual NMR- or X-ray-derived structures [8, 9] further support the notion of highly homologous structures.

Nucleoprotein fibers spread out of cells or plasmid DNA reconstituted with archaeal histones revealed beaded morphology under the electron microscope [3, 10]. Moreover, micrococcal nuclease (MNase) digestion profiles of such fibers exhibited periodicity of cutting [10, 11], superficially similar to that obtained upon digestion of eukaryal chromatin fibers. However, the digestion ladders were very short, and the length of the repeated unit was inferred to be ~60 bp. In our view, this inference raises many questions [3], since the DNA in such particles would have to be severely bent, much more so than in the canonical eukaryal nucleosome, which may represent the limit of possible bending of the rigid DNA double helix [12].

If the particle formed by the binding of HMf to DNA is really so small, the differences among the octamer-

<sup>3</sup>Correspondence: leuba@nih.gov (S.H.L.), jzlatano@duke.poly.edu (J.Z.)

<sup>4</sup>These authors contributed equally to this work.

<sup>5</sup>On leave from the Institute of Biophysics, Academy of Sciences of the Czech Republic, 612 65 Brno, Czech Republic.

<sup>6</sup>On leave from the Research Institute of Physics, St. Petersburg State University, 198904 St. Petersburg, Russia.

**Key words:** atomic force microscope; Archaea; chromatin fibers; HMf; *in vitro* reconstitution; tetrasomes

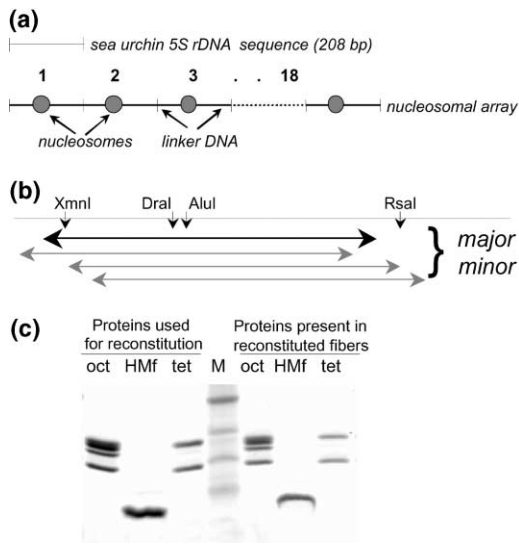


Figure 1. DNA and Proteins Used for In Vitro Chromatin Fiber Reconstitutions

- (a) Schematic of the 208 bp tandemly repeated DNA sequence used as reconstitution substrate.
- (b) Schematic of the major and minor octasome positions within the 208 bp sequence as determined by [32].
- (c) SDS-PAGE analysis of the proteins used for reconstitution or present in reconstituted fibers. Lane M contains protein size markers; lane oct, chicken core histone octamers; lane tet, H3/H4 tetramers; and lane HMf, HMf.

containing eukaryal nucleosomes (hereafter often referred to as octasomes), the H3/H4 tetramer-containing particles (referred to as tetrasomes, following Prunell's nomenclature [13]), and the HMf-containing "nucleosome" will be detectable by AFM imaging. To approach this issue, we have obtained images of nucleoprotein fibers reconstituted on tandemly repeated DNA sequences or on short DNA fragments with either histone octamers, H3/H4 tetramers, or purified HMfs. Various structural parameters were measured on the imaged fibers or individual particles. The AFM-based data were supplemented by results from more conventional biochemical approaches. The combined data clearly demonstrate a very close structural similarity between the canonical eukaryal nucleosomal arrays and those obtained by HMf binding.

## Results

### The 208-12/208-18 Reconstitution System

The majority of the experiments were performed on nucleosomal arrays reconstituted on the tandemly repeated sequence of the 5S rRNA gene from the sea urchin *Lytechinus variegatus* [14]. Each repeat positions a single nucleosome in one (or several closely situated) position(s), thus creating relatively regular fibers on DNA constructs containing 12 or 18 repeats ([14, 15]; Figure 1). The proteins used for reconstitution and those actually present in the reconstitutes are also shown in Figure 1. Chromatin fibers reconstituted on this sequence from eukaryal histones have been extensively characterized by a variety of methods, including AFM [16, 17].

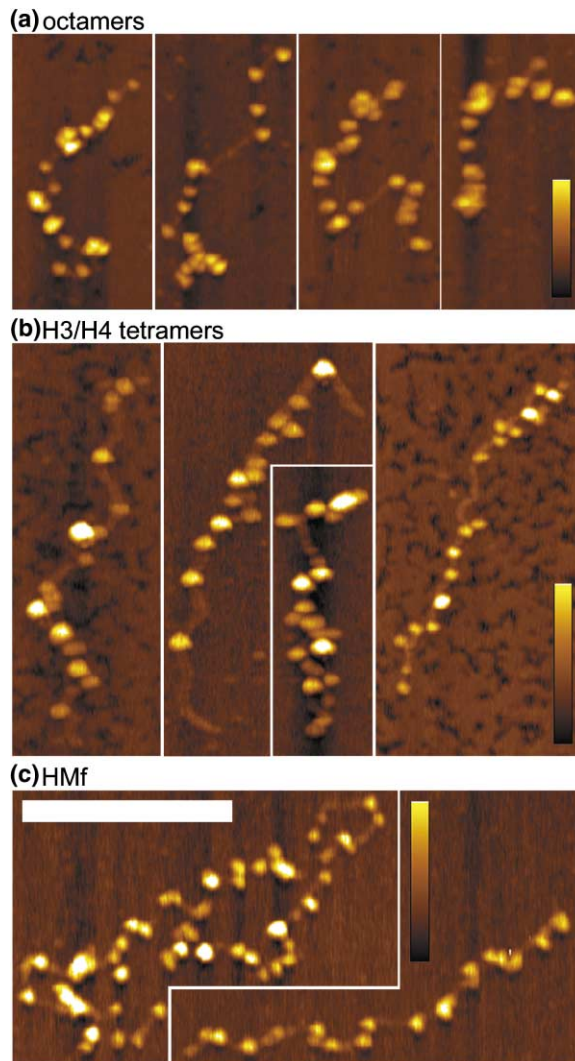


Figure 2. MAC Mode AFM Images of Particle Arrays Reconstituted with Core Histone Octamers, H3/H4 Tetramers, or HMf on the 208-18 DNA Sequence

Heights are coded in color with low areas depicted in dark brown and higher areas depicted in ever-increasingly brighter colors as indicated by the vertical bar. Horizontal bar is 300 nm.

- (a) Control nucleosomal arrays reconstituted with octamers. Heights are on a scale from 0 to 5.5 nm.
- (b) Arrays reconstituted with H3/H4 tetramers. Heights are on a scale from 0 to 4 nm.
- (c) Arrays reconstituted with HMf. Heights are on a scale from 0 to 2.5 nm.

### Particle Arrays Containing HMf: AFM Analysis

Fibers reconstituted on the 5S rDNA sequence were imaged with the AFM, and structural characteristics such as center-to-center interparticle distances and the heights of individual particles within the fibers were measured. Figure 2 presents some typical images of particle arrays reconstituted with octamers, H3/H4 tetramers, and HMfs. All three kinds of fibers looked very similar, with individual particles (nucleosomes) well defined and separated by visible DNA linkers; in fact, it was impossible to distinguish among the three fiber populations in a blind test.

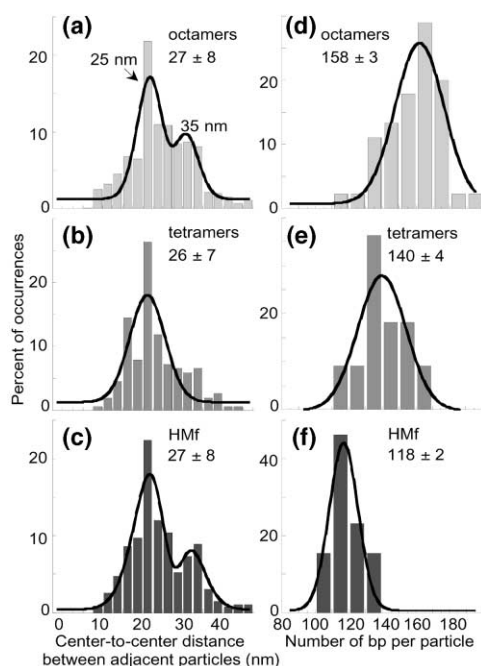


Figure 3. Quantitation of Center-to-Center Distances between Adjacent Particles and Number of Base Pairs per Particle from Fibers in AFM Images

Normalized distributions of distances between centers of adjacent particles (a-c), and number of base pairs per particle in 208-18 reconstituted particle arrays (d-f). Mean center-to-center distances  $\pm$  standard deviations are shown in panels (a-c), with 649, 152, and 853 data points in (a), (b), and (c), respectively. Mean numbers of base pairs per 10 nm of fiber length  $\pm$  standard error are shown in panels (d-f). Gaussian fits to the distributions in (a) and (c) have two maxima at 25 nm and 35 nm (see text). (a) and (d) Control nucleosomal arrays. (b) and (e) Nucleosomal arrays reconstituted with H3/H4 tetramers. (c) and (f) Particle arrays reconstituted with HMf.

Measurements of center-to-center distances (Figures 3a–3c) confirmed the visual impression of profound similarities in fiber structure. Octamer-containing nucleosomal arrays exhibited a bimodal distribution of center-to-center distances (Figure 3a); such a distribution results from occupancy of alternative, closely situated nucleosome positions on successive repeats of the 208 sequence (for detailed analysis of this bimodal distribution, see [18]). Exactly the same type of bimodal distribution was observed on HMf-containing fibers (Figure 3c), again pointing to the close similarities between eukaryal nucleosomal arrays and those containing HMf. The center-to-center distance distribution in H3/H4-containing fibers had a similar mean value, although a bimodal distribution was not obvious. We will come back to this point later.

Next, we calculated the number of base pairs associated with a particle (see Experimental Procedures). The results displayed in Figures 3d–3f show that the means of the frequency distributions were at  $\sim$ 160,  $\sim$ 140, and  $\sim$ 120 bp per particle. It is worth noting that the distributions were somewhat broader for the octamer and tetramer cases than for the HMf case. At a first glance, it may appear that there is a discrepancy in that the center-

to-center distances remain the same for all particle arrays whereas the number of base pairs per particle diminishes from the octasome to the tetrasome to the HMf-containing particle. Reconstitutions on DNA substrates containing multiple repeats of a strong nucleosome positioning sequence are expected to give the same number of particles in all cases (which is what we observed; see Discussion). Then, a change in the length of DNA wrapped around the various protein cores would be expected to give rise to larger center-to-center distances in the case of the smaller particles. This seeming discrepancy results from the way the center-to-center distances were measured: large gaps that may have been due to a missing particle on a given repeat were not measured. On the other hand, these gaps were by necessity included in the contour length measurements that served as the basis for estimating the length of DNA wrapped around individual particles.

Finally, we measured the heights of individual particles within the three kinds of arrays. When chromatin fibers are deposited on mica or glass for imaging, the nucleosomes seem to attach to the surface via the histones, i.e., with their faces down [19]. With such an orientation of nucleosomes on the surface, we would expect a height of  $\sim$ 5 nm for octamer-containing particles [20, 21]. However, heights measured on AFM images of soft biological samples are not absolute [19]; nonetheless, they can legitimately be used for comparative purposes. The data are presented in Figures 4a–4c. As expected from our general knowledge on eukaryal chromatin, the particles containing intact octamers were higher ( $3.7 \pm 0.1$  nm) than those containing tetramers only ( $2.5 \pm 0.1$  nm). The HMf-containing particles were  $\sim$ 2 nm high, and the linker (or naked) DNA was usually in the range of 0.5–0.8 nm high (data not shown). HMf is believed to interact with the DNA as a tetramer [10, 22], so the value for the height of the HMf-containing particle was expected to be closer to that of a eukaryal tetrasome than to that of the octasome. This is exactly what we observed. Since HMf is smaller than H3 or H4 (69 amino acids versus 135 and 102 amino acids, respectively), the height of the HMf-containing particles was smaller,  $\sim$ 2.0 nm. Reassuringly, height values close to those measured on fibers were obtained on monosomal particles (Figures 4d–4f; see also below).

#### Particle Arrays Containing HMf: Nuclease Cleavage Analysis

The presence of nucleosome-like structures in AFM images of HMf-DNA complexes was also confirmed by more conventional biochemical approaches, routinely applied to study eukaryal chromatin [23, 24].

Methidiumpropyl-EDTA-iron(II) (MPE) is a small chemical endonuclease [25] that preferentially hydrolyzes chromatin DNA in the linker regions [26]. Indeed, when nucleosomal arrays reconstituted from DNA and histone octamers were partially cleaved with MPE, a nucleosomal ladder that extended up to 12 nucleosomes was observed on agarose gels (Figure 5a). A very similar ladder was obtained upon MPE cleavage of HMf-containing reconstitutes (Figure 5a), with a seemingly puzzling peculiarity: the ladder never extended far enough

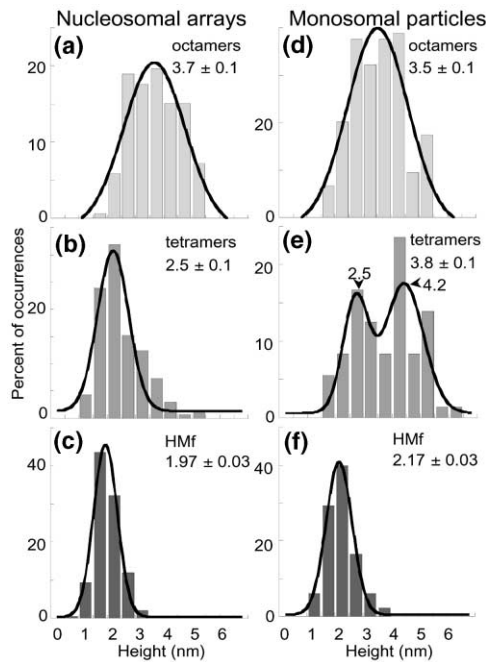


**Figure 4. Quantitation of Heights of Individual Particles from Particle Arrays or Monosomal Particles in AFM Images**

Individual particle heights in 208-18 reconstituted particle arrays (a-c) and monosome particles (d-f). Mean heights  $\pm$  standard errors are shown in all panels, with 153, 138, 193, 149, 74, and 311 data points in (a), (b), (c), (d), (e), and (f), respectively. Gaussian fits to the distributions are also presented.

- (a) Control nucleosomal arrays.
- (b) Arrays reconstituted with H3/H4 tetramers.
- (c) Arrays reconstituted with HMf.
- (d) Control octasomes.
- (e) H3/H4 tetrasomes. Arrowheads point to the maxima at  $\sim$ 2.5 nm and  $\sim$ 4.2 nm (see text).
- (f) HMf-containing monoparticles.

to include the three shortest DNA fragments, corresponding to cleavage down to mono-, di-, and triparticles. It is worth mentioning that the HMf-reconstitute was reproducibly more resistant to digestion than the octamer-containing fiber, but even at levels of digestions which led to the disappearance of the intact 12-mer DNA band on the gel, these small fragments were never observed (see below for discussion).

We next turned to digesting the reconstitutes with MNase. As Figure 5b demonstrates, partial MNase hydrolysis of the linker DNA led to the generation of ladders, similar in appearance for all three protein entities: octamers, H3/H4 tetramers, and HMf. Again, as in the case of MPE digestion, the HMf ladder disappeared below the tri- or tetramer.

Electrophoretic analysis of the MNase digestion products on polyacrylamide gels gave additional information on the structure of the three kinds of fibers. The resolution of these gels is such that intermediate products of digestion are clearly resolved from each other, especially in the region of the gel containing fragments of mono-, di-, and trimers (Figure 5c). As is also clear from the agarose gel in Figure 5b, the octasome-fibers gave a clear-cut periodicity of cleavage, producing fragment ladders covering the entire range from 1 to 12 bands

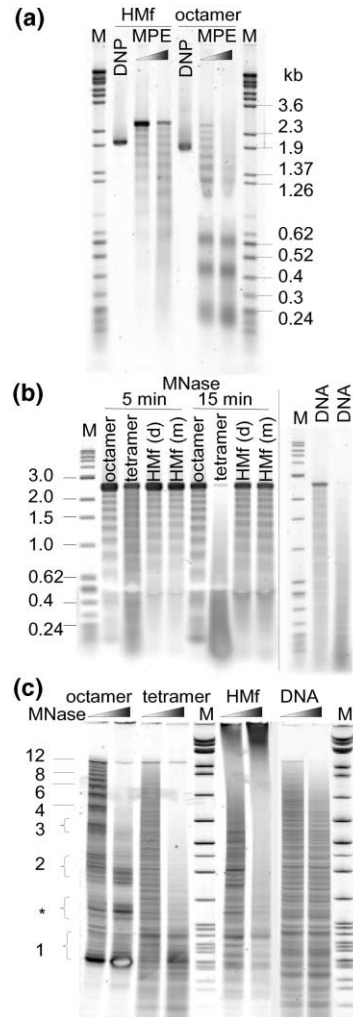


**Figure 5. DNA Products of Partial MPE or MNase Digestions of Octamer-, Tetramer-, and HMf-Containing Particle Arrays Reconstituted on 208-12 DNA**

(a) Partial MPE digestion of octamer- and HMf-containing particle arrays. The triangle denotes increased concentrations of MPE (3 and 6  $\mu$ M). Lane M contains size markers ( $\lambda$ DNA/*Bst*II and pBR322/*Msp*I), and DNP lanes are the respective undigested deoxyribonucleoprotein complexes (loaded without dyes or SDS).

(b) Partial MNase digestion of particle arrays reconstituted on 208-12 DNA. Reconstitutes with core octamers, H3/H4 tetramers, and HMf (the latter prepared either by salt step dialysis [marked d] or by direct mixing [marked m]) were digested with MNase for 5 or 15 min. Size markers (M) are a mixture of the 1 kb DNA ladder and pBR322/*Msp*I. Control digestion of naked DNA is shown in lanes marked "DNA."

(c) MNase digestion pattern as in (b) resolved using 7.5% polyacrylamide gels (1  $\times$  TBE). Numbers indicate the length of the DNA fragments (in the number of repeats) obtained upon digestion of the octasome fiber, with the asterisk denoting fragments that are clearly visible in naked DNA digests, too.

early in digestion. The tetrasome-fiber digestion products, however, were much more evenly distributed throughout the gel, with no clear-cut cleavage periodicity (note also that the tetrasome-fibers produce a much higher background between the ladder bands in the agarose gels). The HMf-containing fibers seemed to occupy an intermediate position between these cases,

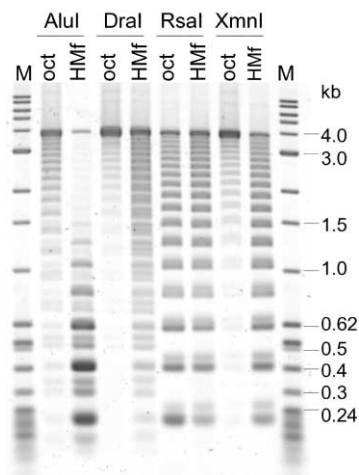


Figure 6. Comparison of Accessibility of Restriction Endonucleases to Reconstituted Octamer and Hmf Arrays on 208-18 DNA

The restriction enzymes are marked above the lanes, and lane M contains size markers (1 kb DNA ladder and pBR322/*Msp*I). The ladders of lighter bands below and above the 208-bp-repeat bands come from cutting within the two end repeats.

with cutting periodicity superior to that in the tetrasome-fiber case but lower than that in the octasome-fiber case. It should be noted, however, that the band patterns for the octamer- and the Hmf-containing fibers were not identical, pointing to differences in the fine organization of the particles in these fibers.

Finally, we used restriction nucleases to see whether they would reveal an interpretable difference between the octasome- and Hmf-fiber structures. We have selected restriction endonucleases that have a single recognition/cutting site within each 208 bp repeat. Cleavage with such enzymes is expected to produce ladders similar to those produced by agents cleaving primarily in linker DNA (MPE, MNase), since the protection provided by a bound protein is never absolute. The relative degree of digestion of the octamer-containing fibers versus the Hmf-containing ones may be used to roughly assess the protection of restriction sites conferred by the presence of the respective protein complexes. Figure 6 presents such a comparison for specific sites protected by the octamer and by Hmf (for the location of the restriction sites on the 208 bp sequence, see Figure 1b).

The *Xmn*I site was rather well protected in the octasome-fiber, as expected from the known nucleosome positions on this sequence (Figure 1b). This site was less well protected in the Hmf-containing fiber. The *Rsa*I site, which is outside the major nucleosome position for the octamer-containing fiber, was well digested on both reconstitutes. The *Rsa*I result may mean that the 208 positioning signal for the octamer serves to also position the Hmf tetramers in accordance with recent results on the general nucleosome-positioning properties of Hmf [27, 28]. Note, however, that Pereira and Reeve [29] state that in their hands the 5S sequence from *L. variegatus* did not position the Hmf particle; this apparent difference from our interpretation could be due to the use of a short 113 bp fragment for reconstitution in that report

(see also below on the use of such short fragments for reconstitution). If the histone octamer and Hmf recognize similar nucleosome-positioning signals, and form, on one and the same sequence, particles with the same dyad position, then the higher accessibility to *Xmn*I cleavage of the Hmf-containing reconstitute would reflect the smaller size of the DNA wrapped around the Hmf core (Figure 3f).

The accessibility of the two reconstituted fibers to *Alu*I and *Dra*I cutting was strongly dependent on whether the fiber contained octamers or Hmfs. These sites are close to the dyad axis of the octamer-containing nucleosome (Figure 1b), and, as expected, they are rather well protected in the octasome fiber (compare degree of digestion of *Alu*I and *Dra*I with *Rsa*I, for instance). With both enzymes, however, the Hmf reconstitute was much more susceptible to cleavage than the octasome fiber. We will discuss this point further, after presenting our results on monosomal particles.

### Hmf-Containing Monosomes: AFM Analysis

To further elucidate the similarities and differences in the structure of the particles created by the different proteins, we performed reconstitution on short DNA fragments that would accommodate a single particle. The reconstitutes on the 208 bp DNA monomer were imaged with the AFM (Figure 7). As can be seen, the individual octasomes or tetrasomes looked very much like their counterparts in the context of the respective fibers (Figure 2). The heights of the monomeric octamer-containing particles were very similar to those measured on fibers. The heights of individual isolated tetrasomes were distributed bimodally, with the two peaks centered at  $\sim 2.5$  nm and  $\sim 4.2$  nm. The first of those peaks corresponded exactly to the value for the tetrasomes in a fiber context (compare Figures 4b and 4e). The second peak of  $\sim 4.2$  nm we attribute to the formation of the so-called ditetrameric nucleosomes which contain two H3/H4 tetramers stacked above each other within the protein core of a single particle [13, 30, 31]. Evidently, ditetrasomes are only formed on monoparticle-sized DNA fragments, since the height distribution in Hmf-containing fibers were narrow, with a single peak of  $\sim 2.5$  nm (Figure 4b).

The AFM images of Hmf-reconstituted monoparticles (Figure 7c) revealed a somewhat unexpected feature. Although in many cases we did observe particles ("nucleosomes"), many of the structures did not possess recognizable particulate morphology; rather, they looked more like stretches of DNA uniformly covered with protein. The heights of the recognizable monoparticles were centered about 2.2 nm (Figure 4f), pretty close to the value measured on individual particles in Hmf fibers (Figure 4c). The heights of the rod-like structures were intermediate between those of the particulate structures and naked DNA ( $\sim 0.5$ – $0.8$  nm under our imaging conditions).

### Monosome Particle Gels Reveal Differences between Eukaryal and Archaeal Particles

The monosome particles organized by the three kinds of protein were next characterized by band-shift analysis using polyacrylamide (Duracryl) gels. The octasomes

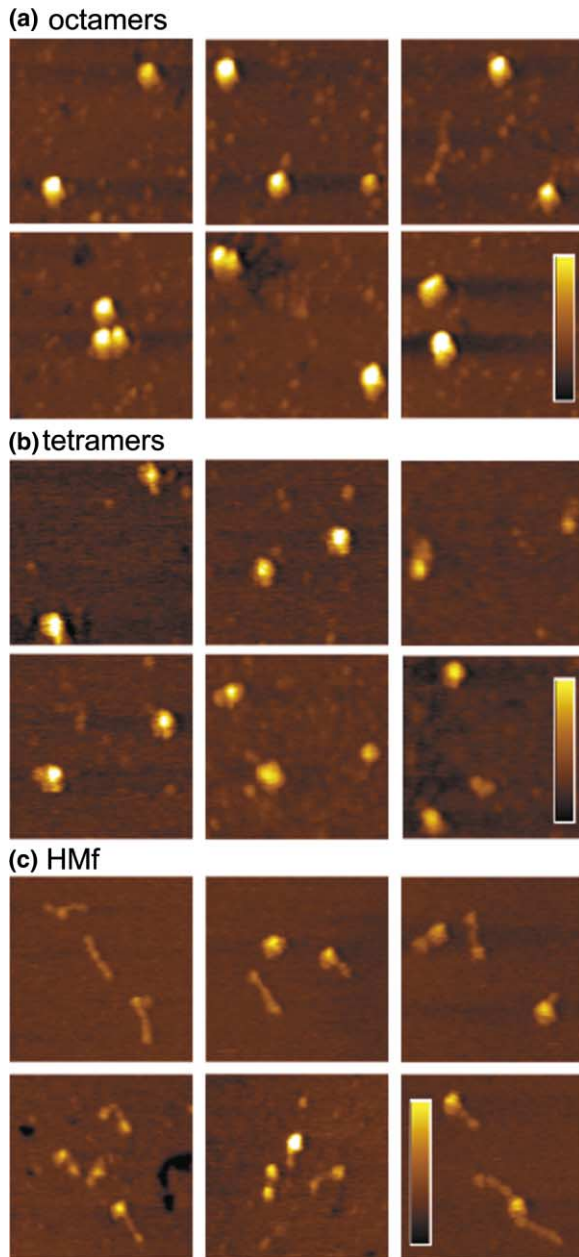


Figure 7. MAC Mode AFM Images of Monoparticles  
(a) Octasomes; height scale from 0 to 4.5 nm.  
(b) H3/H4 tetrasomes; height scale from 0 to 3.5 nm.  
(c) HMf monoreconstitutes; height scale from 0 to 2.5 nm. The size of each square image is  $250 \times 250$  nm.

and tetrasomes reconstituted on a 243 bp 5S sequence produced rather complex patterns of bands, reflecting the presence of several different translational positions on this sequence ([32]; Figure 8a). To our great surprise, only one retarded band was seen in the case of the HMf reconstitute. Careful titration with increasing amounts of HMf again showed only one retarded band that increased in quantity when we increased the amount of protein; in addition, there was considerable amount of material present as a smear between the naked DNA fragment and the retarded band (Figure 8b).

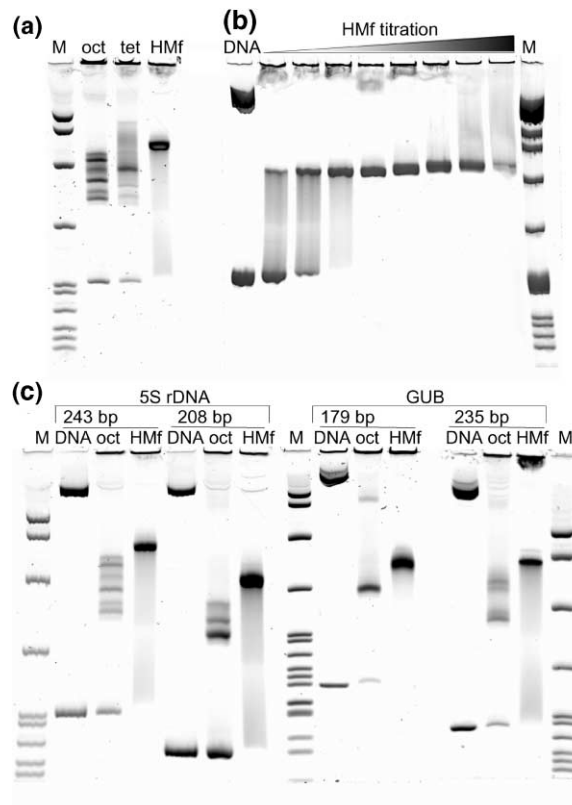


Figure 8. Monosomes Reconstituted with Core Histone Octamers or Tetramers Produce Several DNP Bands on Native Gels, whereas HMf Produces a Single Band Shift

(a) Core octamers, H3/H4 tetramers, and HMf reconstituted on 243 bp 5S rDNA in the presence of the plasmid body. Lane M shows size markers (pBR322/*MspI*).  
(b) Titration of 243 bp 5S rDNA (in the presence of the plasmid body) with HMf.  
(c) Octamers and HMf reconstituted on 243 and 208 bp 5S rDNA and 179 and 235 bp GUB DNA.

To make sure that the appearance of only one retarded band was not dependent on the length and/or on the specific sequence of the DNA fragment used for reconstitution, we performed band-shift analysis by using a shorter piece of the same 5S rDNA sequence or by using a completely unrelated sequence, again in two lengths (Figure 8c). The GUB sequence has been shown to possess a strong nucleosome-positioning signal [33] and has already been used in our laboratory to analyze linker histone binding to reconstituted mononucleosomal particles [34]. Three of the DNA fragments gave the same picture: multiple bands upon octamer reconstitution and a single shifted band (bordering a broad smear) upon HMf binding. The only exception to this behavior was the 179 bp GUB fragment, which gave only one band even with the octamer, probably because it was not long enough to stably accommodate particles with alternative positions (please note that the number of bands on the octasome reconstituted on the 208 bp version of the 5S rDNA sequence was fewer than when the 243 bp version of this sequence was used; compare lanes 6 and 3 in Figure 8c).

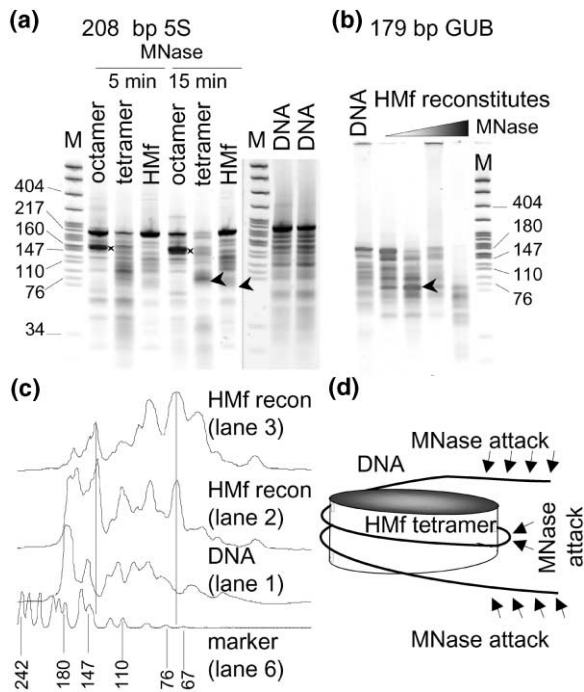


Figure 9. MNase Digestion Products of Monosomal Particles Resolved on 10% PAGE

(a) 208 bp 5S octasomes, H3/H4 tetrasomes, or HMf monomers. Asterisks mark the 146 bp core particle pause (note that the apparent length of this fragment on the gel is  $\sim 160$  bp, due to a slight curvature in the 208 fragment [34, 54]); the arrowheads mark the  $\sim 73$  and  $\sim 70$  bp fragments characteristic of the tetrasomes and HMf monomers, respectively. The right side of the gel is MNase digestion of control naked DNA under very mild conditions of digestion. Digestion conditions used for the reconstituted particles hydrolyze the naked DNA completely.

(b) 179 bp GUB naked DNA (lane 1) and HMf particles (lanes 2–5). Lane M shows size markers (pBR322/*Msp*).

(c) Densitometer traces obtained from fluorescent scans of lanes in (b) (vertical lines denote the  $\sim 70$  and  $\sim 140$  bp DNA fragments present in particle digests only).

(d) Model to explain protection of  $\sim 60$ – $70$  bp DNA fragments by HMf tetramers. Arrows indicate regions of easier accessibility to MNase. Adapted from [35].

### MNase Digestion of Monosome Particles

Why is the band-shift pattern of the HMf-reconstitute so different from that of octasomes? Is there a significant difference in the internal organization of these particles? To understand the structure of the HMf monomer, we analyzed its pattern of digestion with MNase and again compared its digestion pattern with those of octasomes and tetrasomes. As Figure 9a shows, the DNA fragments resulting from cleavage of the 208 octasome revealed the strong “core” particle pause (see asterisks in lanes 2 and 5). In the tetrasome, on the other hand, the core pause was much less well expressed, with a lot of subnucleosomal products quickly accumulating. At later digestion times, a  $\sim 73$  bp fragment became prominent, in agreement with the data of Dong and van Holde [35] on the same sequence, and with earlier reports on random-sequence tetrasomes [36, 37]. The appearance of the  $\sim 73$  bp band in MNase digests of tetrasomes has been attributed to internal cleavage at a position close to the dyad axis of the particle [35].

At first sight, the digestion patterns of the HMf monoreconstitute looked different from both the octasome and the tetrasome (Figure 9a). Since it is known that MNase possesses sequence specificity of cutting [38], and since we knew from the AFM imaging that the HMf monoreconstitute often exhibited rod-like morphology (see Figure 7), we compared the digestion patterns of free DNA to those of the HMf reconstitutes. Indeed, as expected, the two substrates shared a lot of bands (Figure 9). A detailed comparison of the digestion of naked DNA and its HMf-reconstituted counterpart was performed on the GUB 179 bp-fragment (this fragment is devoid of significant intrinsic curvature and behaves normally on polyacrylamide gels, which facilitates the analysis). A representative gel is shown in Figure 9b, and selected traces are shown in Figure 9c. The traces make us appreciate the contribution of the rod-like structures to the pattern and, more importantly, that the HMf-containing particle does produce a prominent band at  $\sim 70$  bp (slightly smaller than the  $\sim 73$  bp fragment in the tetrasome digest) and another band of about twice this length; both of these bands are *not* present in the naked DNA pattern. The appearance of the  $\sim 70$  bp band in the HMf-nucleoprotein complex lends credence to earlier studies reporting MNase digestion products in the range of  $\sim 60$  to  $\sim 70$  bp [11, 27–29]. However, these papers fail to report careful comparisons with naked DNA digestion patterns, and also use relatively short DNA fragments (around or below 100 bp) for reconstitution. Such short fragments may produce anomalous but still stable particles (note that the shortest DNA fragment that produces stable eukaryal nucleosomes is  $\sim 102$  bp [39]). Digestion products larger than  $\sim 60$ – $70$  bp could never be observed when such small fragments are used for reconstitution. For a schematic illustrating the MNase results on HMf-containing particles, see Figure 9d.

Thus, this analysis shows that HMf is capable of organizing even small (monosome-length) fragments into structures very much resembling those organized by H3/H4 tetramers. These particles, though, are in equilibrium with rod-like structures in which the protein seems to uniformly cover the DNA fragment. This observation points to a lesser stability of the HMf particle at the monosome level.

### Discussion

#### HMf Organizes Long Stretches of DNA in Bona Fide Chromatin Fibers

In this work we have used *in vitro* reconstitution to compare the structures of nucleoprotein complexes produced by three different sets of proteins: the histone octamer-containing two molecules each of histones H2A, H2B, H3, and H4, the H3/H4 tetramer, and the archaeal histone HMf. We have used both AFM imaging and quantitations as well as classical nuclease digestion approaches to characterize these reconstituted fibers. The data unequivocally show that HMf is capable of organizing long stretches of DNA in a way very similar to the way nucleosomal arrays are organized by eukaryal histones. The main findings are as follows:

First, HMf-containing nucleoprotein complexes reconstituted on tandemly-repeated eukaryal nucleosome positioning sequences possess morphological features almost indistinguishable from those of eukaryal nucleosomal arrays. Twelve tandem repeats of the positioning sequence produce 11–12 particulate structures in AFM images, and 18 repeats give rise to fibers containing 17–18 particles. The presence of exactly the same number of particles (one particle per repeat) on the three kinds of nucleoprotein reconstitutes is also evidenced by the ladders of digestion with MPE, MNase, and restriction enzymes.

Second, the center-to-center interparticle distances in HMf-containing fibers are exactly the same as in the octamer-containing nucleosomal arrays that are characterized by a bimodal frequency distribution of such distances. Since this bimodal distribution reflects occupancy of alternative nucleosome positions [15, 32] on successive DNA repeats [18], it follows that the HMf protein core recognizes the same major and minor positioning signals as do the octamers. This conclusion is in agreement with recent reports on the general nucleosome positioning properties of HMf [27, 28].

It should be noted here that the tetrasome fibers exhibited a very similar mean of the center-to-center distance distributions (Figure 3b), but two peaks were not easily discernable. This could mean that the H3/H4 tetramers, although reportedly recognizing nucleosome-positioning sequences by themselves (e.g., [31, 35]), do so less rigorously than does the complete octamer. Alternatively, the long-range organization induced by the H3/H4 tetramer is relatively easily disrupted by MNase, as suggested earlier [36]. Indeed, the results of MNase digestion on 208-12 DNA reconstitutes do indicate that the tetrasome fibers produce much more diffuse ladders than do the octasome fibers (Figure 5). The MNase ladder on polyacrylamide gels (Figure 5c), while very well expressed in the octasome fibers, is actually difficult to discern in the tetrasome fibers; the pattern for the HMf fibers is actually closer to that of the octasome fiber, in agreement with the center-to-center distance distributions in Figure 3.

Third, the structural properties of individual particles (octasome, tetrasome, and HMf-containing) can be deduced from the measurements of some parameters in AFM images. Thus, particle heights, whether measured at the fiber level or at the level of monparticles, are greatest in octasomes, intermediate in tetrasomes, and least in HMf-containing particles (Figure 4). This is exactly what is expected on the basis of the known composition (number and size of proteins) of the protein cores of the respective particles.

Another interesting structural parameter of the individual particles is the number of base pairs of DNA associated with the protein cores. As Figure 3 shows, the octamer organizes ~160 bp, the tetramer, ~140 bp, and the HMf, ~120 bp of DNA. These numbers are only approximate (see Experimental Procedures for an explanation of how the measurements were done) and may actually slightly overestimate the respective lengths. It is reassuring to see that our AFM measurements do reflect (albeit in relative, not absolute terms) the biochemically-derived DNA lengths organized by complete

octasomes versus tetrasomes (146 bp versus 120 bp, respectively; [36, 40, 41]).

Fourth, the internal organization and stability of the HMf-containing particle is of great interest. From the HMf fiber data, it seems clear that HMf organizes a shorter piece of DNA even in comparison with the H3/H4 tetramer (see above). The results from MNase digestion of monosomal particles organized by octamers, H3/H4 tetramers, and HMf are instructive in this respect. As Figure 9 shows, while the octasome clearly exhibits the core particle intermediate digestion product, this product is barely distinguishable both in the tetramer- and HMf particle-digestion patterns; moreover, both the tetrasome and HMf-particle produce major DNA fragments in the subnucleosomal region. For the tetrasome, this fragment is ~73–74 bp (see also [35]) and for the HMf particle, ~70 bp. The appearance of such a fragment in the tetrasome has been attributed to internal cleavage at a position close to the dyad axis of the particle [35], an interpretation supported by the crystal structure of the octasome, namely by the internal location of the different histones within the particle [20, 21]. The absence of the H2A/H2B dimers in a particle would expose the dyad axis to nucleolytic attack. The presence of a subnucleosomal fragment of similar length in the HMf particle digest argues that the internal organization of this particle is very similar to that of the tetrasome, in agreement with reports from Reeve's laboratory of the tetrameric structure of the HMf protein core in archaeal chromatin [2, 3, 22].

The data on the restriction nuclease digestion of the 208-12 reconstitutes (Figure 6) confirm the notion that HMf-containing particles have their dyad axes rather well exposed to nucleolytic cleavage. The two restriction endonucleases, *AluI* and *DraI*, whose cutting sites lie close to the dyad axis of the major nucleosome position in the octasome (see Figure 1), digest the HMf fiber much more avidly than the octasome fiber.

Finally, the HMf monparticles seem to be much more unstable than the octasomes or tetrasomes. The former exist in equilibrium with rod-like structures, as evidenced by both the AFM images in Figure 7 and by the MNase digestion pattern in Figure 9. The digestion pattern of HMf reconstitutes on short, monosome-length DNA fragments is actually a superimposition of a monparticle pattern and that of naked DNA. This lower stability of the HMf monparticles may easily explain the “disappearance” of mono-, di-, tri-, and even tetraparticle DNA fragments in both MPE and MNase digestion patterns of long fibers (see Figure 5). Once these long fibers are digested down to a certain length (four or fewer particles), the resulting intermediate digestion products are unstable and, hence, cannot be observed. We may speculate that in the eukaryal nucleosome the DNA wrapped around the histone octamer is, in a way, “locked” into place by the core histone tails extruding through the aligned minor grooves of the neighboring DNA gyres [20, 21]. The HMf particle cannot be stabilized in a similar way because of the lack of these random-coiled tails.

Fifth, the organization of the HMf-containing particle shows some features that distinguish it from both the octasome and the tetrasome. Interestingly, band-shift

analysis using two completely different sequences of two lengths each never revealed more than one shifted band produced by HMf binding. This is in sharp contrast to the band-shift patterns produced by histone octamer or H3/H4 tetramer binding to the same sequences, where multiple bands were observed (note an exception with the octamer binding to the 179 bp GUB sequence, where only one shifted band was seen with the octamer). The presence of multiple band-shifts in such DNP gels has been interpreted as reflecting the presence of several alternative translational nucleosome positions in each DNA repeat in the context of the 18 octasome fiber [15, 32]. The presence of several such positions within each repeat is probably also characteristic of the HMf fiber (see above). Further detailed high-resolution analysis of the positioning properties of HMf on monoparticle-sized DNA fragments will be needed to resolve this puzzle.

### Biological Implications

We believe that the data presented here convincingly show that the *in vitro* structure of reconstituted chromatin fibers containing eukaryal or archaeal histone is very similar. The detailed analysis of these fibers support previous reports on the existence of chromatin in Archaea and resolve some of the important structural issues that still remained unanswered by those reports (see Introduction). The unambiguous existence of archaeal chromatin also supports the ideas of Carl Woese about the evolution of life on Earth.

In eukaryotes, the needs for regulation of transcriptional activity are much more complex than the needs in the simpler unicellular archaeal organisms. The need for fine-tuning transcription may have led to the evolutionary appearance and conservation of the core histone tails that carry the postsynthetic modification information. The HMf protein encompasses the three helices of the histone-fold motif only and thus completely lacks the N-terminal tails of the eukaryal core histones. The histone tails in eukaryal chromatin may have a dual function: to stabilize the nucleosomal particles locking the DNA in place and to loosen the structure in a highly regulatable manner through postsynthetic modifications.

### Experimental Procedures

#### Purification of DNA and Histones

All restriction enzymes were from New England Biolabs. 208-12 and 208-18 DNAs were prepared by *Hin*PI digestion of plasmid pPoll208 [42] and pT207-18, a kind gift of Dr. P. Yau [43], respectively. Subsequent digestion of 208-12 DNA by *Ava*I produced 208 bp DNA. A 243 bp fragment was obtained from pMSA-3 plasmid [34] after digestion with *Bam*HI as well as 179 bp GUB DNA from pGUB [33]. GUB fragments (235-bp-long) were digested out of pBSGUB (plasmid construction in [34]) with *Hind*III and *Eco*RI.

DNA fragments were purified by gel filtration using Ultrogel A2 (Biosepra) 60 × 1.6 cm column in 0.5 M NaCl, 25 mM Tris-HCl (pH 7.5), and 0.5 mM EDTA. Chicken core histone octamers and H3/H4 tetramers were purified from frozen packed chicken erythrocytes (Pel Freeze) using hydroxyapatite chromatography [44]. Purity and stoichiometry were analyzed by sodium dodecyl sulfate (SDS) polyacrylamide gel electrophoresis (PAGE) [45]. Recombinant HMfB [46] was a kind gift from Dr. J. Reeve.

#### Chromatin Reconstitution and Characterization

Chromatin reconstitution was performed by salt dialysis [47] using a 1:1 weight ratio of DNA to histone octamers or HMf and 2:1 weight ratio of DNA to H3/H4 tetramers. Samples in 2 M NaCl were successively dialyzed against 1 M, 0.75 M, and 0 M NaCl solution buffered with 10 mM triethanolamine (TEA)-HCl (pH 7.5), by using Slide-A-Lyzer minidialysis units (Pierce). Each dialysis step was carried out for at least 3 hr, the last one usually for 9 hr.

H3/H4 tetramer reconstitution was also performed by reconstituting octamers and then by washing the octamer reconstitute with 1 M NaCl, 10 mM TEA-HCl (pH 7.5) (three times) using Microcon 100 (Millipore), followed by three washes with 10 mM TEA-HCl (pH 7.5). This was done to make sure that the tetrasome-fibers contained only one H3/H4 tetramer per particle, and not two [30, 31]. No differences in chromatin fiber structure between these two H3/H4 tetramer reconstitution methods were detected at the fiber level by AFM, Mnase, or MPE.

HMf reconstitutes were also prepared by direct mixing of HMf and DNA in 50 mM Tris-HCl (pH 8.0) and 100 mM KCl and subsequent dialysis to 10 mM TEA-HCl (pH 7.5); direct mixing protocols have been used in J. Reeve's laboratory, so we performed such reconstitutions for comparative purposes.

Monosomes were reconstituted by the step-dilution method [48] starting from ~10  $\mu$ l of solution of DNA (0.2  $\mu$ g/ $\mu$ l in 2 M NaCl, 10 mM TEA-HCl [pH 7.5]). Samples were incubated at 37°C for 20 min, diluted with one volume of 10 mM TEA-HCl (pH 7.5) to 1 M NaCl, incubated for another 20 min, diluted to 0.75 M NaCl, and finally diluted to 0.5 M NaCl. Dialysis using 0.025  $\mu$ m pore-size Millipore membranes floating on 10 mM TEA-HCl (pH 7.5) or Slide-A-Lyzer minidialysis units was done at 4°C for 2 hr.

The quality of all reconstitutes was checked by MPE hydrolysis [25, 26, 49]. The reaction was performed for 10 min in 10  $\mu$ l, using freshly prepared MPE-Fe complex and stopped by adding 4 × SDS-loading buffer containing 20 mM bathophenanthrolinedisulfonic acid (Sigma). Samples were electrophoresed on a 1.6% agarose gel in 1 × TAE. Gels were stained with SYBR Green (Molecular Probes) and washed in water prior to scanning using the blue fluorescence setting on Storm 860 (Molecular Dynamics).

Restriction enzyme digestions were performed with ~0.5  $\mu$ g of sample and 10 units of enzyme for 2 hr. Reactions were stopped by 20 mM EDTA and 0.1% SDS with 100  $\mu$ g/ml proteinase K and run on agarose gels, as in the case of MPE.

For MNase digestions, 1–5 units of MNase (Worthington) were added to 8–9  $\mu$ l (~0.5  $\mu$ g) of reconstitute or DNA and incubated at 37°C for 5–30 min. The reaction was stopped by adding 4 × SDS-loading buffer, which contained 50 mM EDTA. Agarose gel electrophoresis and subsequent analysis was as in the case of MPE. Prior to analyzing the samples on PAGE, samples were treated with proteinase K, phenol/chloroform was extracted, and ethanol was precipitated.

Monosome reconstitutions were examined by band-shift PAGE, usually on 10-cm-long slab gels, with 5% or 5.5% Duracryl (30:0.8 acryl:bis) (Genomic Solutions) gel poured in TBE/3. The gels were stained and analyzed in the same way as the agarose gels described above.

#### AFM Imaging and Analysis

Particle arrays and monosomes (absorbance of 1–2 at  $\lambda = 260$  nm) in 10 mM TEA-HCl (pH 7.5), 0.1 mM EDTA were fixed with 0.1% glutaraldehyde overnight. Fixation was done to avoid possible effects of shearing forces during deposition on the surface and the subsequent washing step [50]. Sample (2  $\mu$ l) was deposited on freshly cleaved mica for 1–5 min, rinsed with 5–10 drops of Milli-Q (Millipore) water, and fluxed with argon to remove the visible layer of liquid [51]. Imaging was performed on a MAC Mode AFM (Molecular Imaging, Phoenix, AZ), using magnetically coated silicon nitride probes oscillated above the surface at a frequency of ~100 kHz. The amplitude of oscillation was kept constant during the scanning by piezo height compensation. Each set of experiments was repeated at least three times, using, whenever possible, the same tip for the three different kind of samples. Using the same tip equalizes the broadening effect of the tip over images to be directly compared.

Center-to-center distances between adjacent particles were mea-

sured as described [19, 52]. Two particles in the same fiber were considered to be adjacent only if there was not sufficient distance to place a nucleosome between them. Hence, large gaps are not reflected in the center-to-center measurements. Measurements were repeated on different days on the same data set, and the same results were obtained. Only fibers clearly separated from other fibers were selected for measuring the number of base pairs per particle. This parameter was determined according to the following formula: number of base pairs per particle =  $((1273 - l)/N)/0.34$ . Where 1273 nm is the contour length of the 208-18 DNA in B form,  $l$  is the measured fiber length from the image,  $N$  is the number of particles in the measured fiber, and 0.34 nm is the distance between base pairs in double helical DNA [53]. Note that such a measurement is based on the apparent reduction in the DNA contour length due to particle formation, and does not take into account any geometrical considerations; thus, it is only an approximate measure for the number of bp of DNA wrapped about the protein core.

#### Acknowledgments

We thank Dr. J. Reeve for the gift of HMf, Dr. P. Yau for the gift of pT207-18, and Dr. J. Workman for the gift of pGUB. S.H.L. is a National Cancer Institute Scholar.

Received: June 12, 2001

Revised: October 3, 2001

Accepted: November 5, 2001

#### References

1. Woese, C.R., Kandler, O., and Wheelis, M.L. (1990). Towards a natural system of organisms: proposal for the domains Archaea, Bacteria, and Eucarya. *Proc. Natl. Acad. Sci. USA* **87**, 4576–4579.
2. Reeve, J.N., Sandman, K., and Daniels, C.J. (1997). Archaeal histones, nucleosomes, and transcription initiation. *Cell* **89**, 999–1002.
3. Zlatanova, J. (1997). Archaeal chromatin: virtual or real? *Proc. Natl. Acad. Sci. USA* **94**, 12251–12254.
4. Bult, C.J., et al., and Venter, J.C. (1996). Complete genome sequence of the methanogenic archaeon, *Methanococcus jannaschii*. *Science* **273**, 1058–1073.
5. Grayling, R.A., Sandman, K., and Reeve, J.N. (1996). Histones and chromatin structure in hyperthermophilic Archaea. *FEMS Microbiol. Rev.* **18**, 203–213.
6. Arents, G., and Moudrianakis, E.N. (1995). The histone fold: a ubiquitous architectural motif utilized in DNA compaction and protein dimerization. *Proc. Natl. Acad. Sci. USA* **92**, 11170–11174.
7. Baxevasis, A.D., Arents, G., Moudrianakis, E.N., and Landsman, D. (1995). A variety of DNA-binding and multimeric proteins contain the histone fold motif. *Nucleic Acids Res.* **23**, 2685–2691.
8. Starich, M.R., Sandman, K., Reeve, J.N., and Summers, M.F. (1996). NMR structure of HMfB from the hyperthermophile, *Methanothermus fervidus*, confirms that this archaeal protein is a histone. *J. Mol. Biol.* **255**, 187–203.
9. Decanniere, K., Babu, A.M., Sandman, K., Reeve, J.N., and Heinemann, U. (2000). Crystal structures of recombinant histones HMfA and HMfB from the hyperthermophilic archaeon *Methanothermus fervidus*. *J. Mol. Biol.* **303**, 35–47.
10. Pereira, S.L., Grayling, R.A., Lurz, R., and Reeve, J.N. (1997). Archaeal nucleosomes. *Proc. Natl. Acad. Sci. USA* **94**, 12633–12637.
11. Grayling, R.A., Bailey, K.A., and Reeve, J.N. (1997). DNA binding and nuclease protection by the HMf histones from the hyperthermophilic archaeon *Methanothermus fervidus*. *Extremophiles* **1**, 79–88.
12. Hagerman, P.J. (1988). Flexibility of DNA. *Annu. Rev. Biophys. Chem.* **17**, 265–286.
13. Allat, M., Sivolob, A., Revet, B., and Prunell, A. (1999). Nucleosome dynamics. Protein and DNA contributions in the chiral transition of the tetrasome, the histone (H3–H4)<sub>2</sub> tetramer-DNA particle. *J. Mol. Biol.* **291**, 815–841.
14. Simpson, R.T., Thoma, F., and Brubaker, J.M. (1985). Chromatin reconstituted from tandemly repeated cloned DNA fragments and core histones: a model system for study of higher order structure. *Cell* **42**, 799–808.
15. Pennings, S., Meersseman, G., and Bradbury, E.M. (1991). Mobility of positioned nucleosomes on 5S rDNA. *J. Mol. Biol.* **220**, 101–110.
16. Allen, M.J., et al., and Bradbury, E.M. (1993). Atomic force microscope measurements of nucleosome cores assembled along defined DNA sequences. *Biochemistry* **32**, 8390–8396.
17. Leuba, S.H., et al., and Lindsay, S.M. (2000). The mechanical properties of single chromatin fibers under tension. *Single Mol.* **1**, 185–192.
18. Karymov, M.A., Tomschik, M., Leuba, S.H., Caiafa, P., and Zlatanova, J. (2001). DNA methylation-dependent chromatin fiber compaction *in vivo* and *in vitro*: requirement for linker histone. *FASEB J.* **15**, 2631–2641.
19. Leuba, S.H., Bustamante, C., Zlatanova, J., and van Holde, K. (1998). Contributions of linker histones and histone H3 to chromatin structure: scanning force microscopy studies on trypsinized fibers. *Biophys. J.* **74**, 2823–2829.
20. Luger, K., Mader, A.W., Richmond, R.K., Sargent, D.F., and Richmond, T.J. (1997). Crystal structure of the nucleosome core particle at 2.8 Å resolution. *Nature* **389**, 251–260.
21. Harp, J.M., Hanson, B.L., Timm, D.E., and Bunick, G.J. (2000). Asymmetries in the nucleosome core particle at 2.5 Å resolution. *Acta Crystallogr. D* **56**, 1513–1534.
22. Bailey, K.A., Chow, C.S., and Reeve, J.N. (1999). Histone stoichiometry and DNA circularization in archaeal nucleosomes. *Nucleic Acids Res.* **27**, 532–536.
23. van Holde, K.E. (1988). *Chromatin*. (New York: Springer-Verlag).
24. Tsanev, R., Russev, G., Pashev, I., and Zlatanova, J. (1992). *Replication and Transcription of Chromatin*. (Boca Raton: CRC Press).
25. Hertzberg, R.P., and Dervan, P.B. (1984). Cleavage of DNA with methidiumpropyl-EDTA-iron(II): reaction conditions and product analyses. *Biochemistry* **23**, 3934–3945.
26. Cartwright, I.L., and Elgin, S.C. (1989). Nonenzymatic cleavage of chromatin. *Methods Enzymol.* **170**, 359–369.
27. Sandman, K., and Reeve, J.N. (1999). Archaeal nucleosome positioning by CTG repeats. *J. Bacteriol.* **181**, 1035–1038.
28. Bailey, K.A., Pereira, S.L., Widom, J., and Reeve, J.N. (2000). Archaeal histone selection of nucleosome positioning sequences and the prokaryotic origin of histone-dependent genome evolution. *J. Mol. Biol.* **303**, 25–34.
29. Pereira, S.L., and Reeve, J.N. (1999). Archaeal nucleosome positioning sequence from *Methanothermus fervidus*. *J. Mol. Biol.* **289**, 675–681.
30. Flaus, A., Luger, K., Tan, S., and Richmond, T.J. (1996). Mapping nucleosome position at single base-pair resolution by using site-directed hydroxyl radicals. *Proc. Natl. Acad. Sci. USA* **93**, 1370–1375.
31. Spangenberg, C., et al., and Beato, M. (1998). The mouse mammary tumour virus promoter positioned on a tetramer of histones H3 and H4 binds nuclear factor 1 and OTF1. *J. Mol. Biol.* **278**, 725–739.
32. Meersseman, G., Pennings, S., and Bradbury, E.M. (1991). Chromatinosome positioning on assembled long chromatin. Linker histones affect nucleosome placement on 5S rDNA. *J. Mol. Biol.* **220**, 89–100.
33. Adams, C.C., and Workman, J.L. (1995). Binding of disparate transcriptional activators to nucleosomal DNA is inherently cooperative. *Mol. Cell. Biol.* **15**, 1405–1421.
34. An, W., Leuba, S.H., van Holde, K., and Zlatanova, J. (1998). Linker histone protects linker DNA on only one side of the core particle and in a sequence-dependent manner. *Proc. Natl. Acad. Sci. USA* **95**, 3396–3401.
35. Dong, F., and van Holde, K.E. (1991). Nucleosome positioning is determined by the (H3–H4)<sub>2</sub> tetramer. *Proc. Natl. Acad. Sci. USA* **88**, 10596–10600.
36. Camerini-Otero, R.D., Sollner-Webb, B., and Felsenfeld, G. (1976). The organization of histones and DNA in chromatin: evidence for an arginine-rich histone kernel. *Cell* **8**, 333–347.
37. Read, C.M., Baldwin, J.P., and Crane-Robinson, C. (1985).

- Structure of subnucleosomal particles. Tetrameric (H3/H4)<sub>2</sub> 146 base pair DNA and hexameric (H3/H4)<sub>2</sub>(H2A/H2B)<sub>1</sub> 146 base pair DNA complexes. *Biochemistry* 24, 4435–4450.
38. McGhee, J.D., and Felsenfeld, G. (1983). Another potential artifact in the study of nucleosome phasing by chromatin digestion with micrococcal nuclease. *Cell* 32, 1205–1215.
  39. van Holde, K., and Zlatanova, J. (1999). The nucleosome core particle: does it have structural and physiologic relevance? *Bioessays* 21, 776–780.
  40. Hayes, J.J., Clark, D.J., and Wolffe, A.P. (1991). Histone contributions to the structure of DNA in the nucleosome. *Proc. Natl. Acad. Sci. USA* 88, 6829–6833.
  41. Hayes, J.J., and Wolffe, A.P. (1992). Histones H2A/H2B inhibit the interaction of transcription factor IIIA with the *Xenopus borealis* somatic 5S RNA gene in a nucleosome. *Proc. Natl. Acad. Sci. USA* 89, 1229–1233.
  42. Georgel, P., Demeler, B., Terpening, C., Paule, M.R., and van Holde, K.E. (1993). Binding of the RNA polymerase I transcription complex to its promoter can modify positioning of downstream nucleosomes assembled in vitro. *J. Biol. Chem.* 268, 1947–1954.
  43. O'Neill, T.E., Roberge, M., and Bradbury, E.M. (1992). Nucleosome arrays inhibit both initiation and elongation of transcripts by bacteriophage T7 RNA polymerase. *J. Mol. Biol.* 223, 67–78.
  44. von Holt, C., et al., and Sewell, B.T. (1989). Isolation and characterization of histones. *Methods Enzymol.* 170, 431–523.
  45. Laemmli, U.K. (1970). Cleavage of structural proteins during the assembly of the head of bacteriophage T4. *Nature* 227, 680–685.
  46. Sandman, K., Grayling, R.A., and Reeve, J.N. (1995). Improved N-terminal processing of recombinant proteins synthesized in *Escherichia coli*. *Biotechnology* 13, 504–506.
  47. Tatchell, K., and van Holde, K.E. (1977). Reconstitution of chromatin core particles. *Biochemistry* 16, 5295–5303.
  48. Zivanovic, Y., Duband-Goulet, I., Schultz, P., Stofer, E., Oudet, P., and Prunell, A. (1990). Chromatin reconstitution on small DNA rings. III. Histone H5 dependence of DNA supercoiling in the nucleosome. *J. Mol. Biol.* 214, 479–495.
  49. Zlatanova, J., Leuba, S.H., Yang, G., Bustamante, C., and van Holde, K. (1994). Linker DNA accessibility in chromatin fibers of different conformations: a reevaluation. *Proc. Natl. Acad. Sci. USA* 91, 5277–5280.
  50. Leuba, S.H., et al., and Bustamante, C. (1994). Three-dimensional structure of extended chromatin fibers as revealed by tapping-mode scanning force microscopy. *Proc. Natl. Acad. Sci. USA* 91, 11621–11625.
  51. Leuba, S.H., and Bustamante, C. (1999). Analysis of chromatin by scanning force microscopy. *Methods Mol. Biol.* 119, 143–160.
  52. Leuba, S.H., Bustamante, C., van Holde, K., and Zlatanova, J. (1998). Linker histone tails and N-tails of histone H3 are redundant: scanning force microscopy studies of reconstituted fibers. *Biophys. J.* 74, 2830–2839.
  53. Dickerson, R.E. (1983). The DNA helix and how it is read. *Sci. Am.* 249, 94–111.
  54. Dong, F., Hansen, J.C., and van Holde, K.E. (1990). DNA and protein determinants of nucleosome positioning on sea urchin 5S rRNA gene sequences in vitro. *Proc. Natl. Acad. Sci. USA* 87, 5724–5728.